Nonlinear resonances and energy transfer in finite granular chains

Joseph Lydon,[1,2] Georgios Theocharis,[3] and Chiara Daraio[1,2,*]

[1]*Graduate Aerospace Laboratories (GALCIT), California Institute of Technology, Pasadena, California 91125, USA*

[2]*Department of Mechanical and Process Engineering, Swiss Federal Institute of Technology (ETH), Zürich, Switzerland*

[3]*LAUM, UMR-CNRS 6613, Université du Maine, Avenue O. Messiaen, 72085 Le Mans, France*

(Received 25 November 2013; revised manuscript received 20 October 2014; published 19 February 2015)

In the present work we test experimentally and compute numerically the stability and dynamics of harmonically driven monoatomic granular chains composed of an increasing number of particles N ($N = 1$–50). In particular, we investigate the inherent effects of dissipation and finite size on the evolution of bifurcation instabilities in the statically compressed case. The findings of the study suggest that the nonlinear bifurcation phenomena, which arise due to finite size, can be useful for efficient energy transfer away from the drive frequency in transmitted waves.

DOI: 10.1103/PhysRevE.91.023208 PACS number(s): 45.20.D−, 45.70.−n, 46.40.Cd

I. INTRODUCTION

Acoustic imaging, sensing, energy harvesting, and communication all rely on a firm understanding of the physics of wave propagation and energy transport. To advance these and other applications and to create new materials with enhanced acoustic properties, phononic crystals and acoustic metamaterials have been extensively studied [1,2]. These are a class of engineered or structured materials that allow control over wave propagation properties by exploiting geometry and periodicity of subwavelength structures. One important consequence of periodicity in an infinite material is the presence of frequency band gaps, which results in the complete reflection of excitations with frequencies in the band gap. In reality, all materials are inherently finite, dissipative, and not completely periodic. In systems with finite size, nonlinear instabilities become increasingly more important, even for relatively small dynamic excitations. In this work, we study the nonlinear dynamic phenomena that result from finite size, while considering dissipation. The presence of these nonlinear effects in a finite system could be very useful in the design of phononic crystals and metamaterials for practical applications.

To further advance the development of acoustic materials, the complex behavior of nonlinear media offers enhanced (i.e., amplitude and frequency dependent) control over the wave propagation. By introducing nonlinear responses in the design of materials, it is possible to control acoustic propagation properties, achieve greater tunability on the acoustic response of given systems, and observe new physical phenomena. For example, nonlinear systems have a distinct advantage over linear systems in their ability to transfer energy between frequencies. Common examples of energy transfer in the frequency domain are subharmonic and superharmonic bifurcations [3]. While these bifurcations can be destructive and are oftentimes avoided (as suggested by von Karman in the design of parts in an airplane [4]), they are also frequently engineered into systems, e.g., sum-frequency and second harmonic generation in nonlinear optics devices [5]. In acoustics, this nonlinear transfer of energy resulted in the development of rectification devices [6,7] and has been used in nondestructive evaluation and imaging techniques [8].

In this work, we study the propagation of energy in finite periodic systems that results from similar nonlinear processes, in which energy is exchanged between different frequencies of the system. As mentioned above, in linear periodic materials excitations in the band gap are completely reflected. However, the presence of nonlinearity allows energy to propagate down the chain. This can occur through nonlinear supratransmission in which the energy of a signal in the frequency band gap is transmitted by means of nonlinear modes [9–11]. This is shown in a series of papers investigating nonlinear supratransmission in sine-Gordon and Klein-Gordon [12], Josephson ladders [9], and Fermi-Pasta-Ulam chains [10]. Here, we explore similar nonlinear phenomena in systems of finite size. We accomplish this by studying granular chains of particles as fundamental models for nonlinear periodic structures. We study the bifurcations arising in these systems, and we explore the transition regime bridging the response of finite systems with theoretical predictions based on infinite periodic assumptions.

Granular chains are a class of nonlinear periodic media governed by a highly tunable Hertzian contact interaction between particles [13]: this allows the system to access near-linear, weakly nonlinear, and strongly nonlinear dynamic behavior [14]. In the weakly nonlinear regime, the granular chains' dynamics are similar to Fermi-Pasta-Ulam systems, and they have demonstrated defect energy localization [15], discrete breathers [16,17], higher order harmonic wave generation [18], as well as chaotic dynamics [19]. In the highly nonlinear regime, coherent traveling waves were predicted to exist such as highly localized solitary waves [14] and periodic traveling waves [20]. Granular chains have been suggested for application in tunable mechanical filtering [21] and acoustic rectification [6]. In the field of dense granular materials, frequency-mixing processes have been reported for elastic waves [22]. Their experimental tractability makes granular chains excellent platforms for studying lattice dynamics with highly dependent amplitude and frequency behavior. In addition, the granular chain is an ideal model to study phenomena that occur across different dynamical regimes. When the dynamics are weakly nonlinear and smooth the granular interaction potential can be approximated by a

*Corresponding author: daraio@ethz.ch

polynomial expansion. This extends the applicability of the results in this regime to similar lattice systems with weak nonlinearities. We demonstrate that the bifurcations presented occur both in the smooth weakly nonlinear regime and also the strongly nonlinear regime, in which gaps open between beads.

II. EXPERIMENTAL SETUP

Figure 1(a) shows a schematic of the experimental setup. We assemble a one-dimensional (1D) homogeneous granular chain made of N stainless steel spheres (316 type, grade 100, provided by McMaster-Carr). The spheres have a measured radius $R = 9.525$ mm, measured mass $m = 28.84$ g, Youngs modulus $E = 193$ GPa, and Poisson ratio $\nu = 0.3$ [23]. We excite the system with a harmonic displacement for approximately 400 ms, enough time to reach stationary dynamics, using a low voltage piezoelectric actuator (blocking force 800 N, resonance frequency 40 kHz, PST 150/5/7 VS10 provided by Piezomechanik). The actuator is mounted on a steel block fixed to the table. N spheres (with N ranging between 1 and 50) are then aligned with the head of the actuator and supported by polycarbonate rods. We excite with a range of static and dynamic loading that allows access to both the weakly and strongly nonlinear dynamical regime. We use a noncontact laser vibrometer to measure the dynamic response of the short granular systems (i.e., $N \leqslant 2$) at the last bead, ensuring no effects of the measurement system on the results. In longer systems, we use calibrated sensor particles, placed in the third and last bead, similar to Job *et al.* [24]. The applied static load is measured using a calibrated static force sensor.

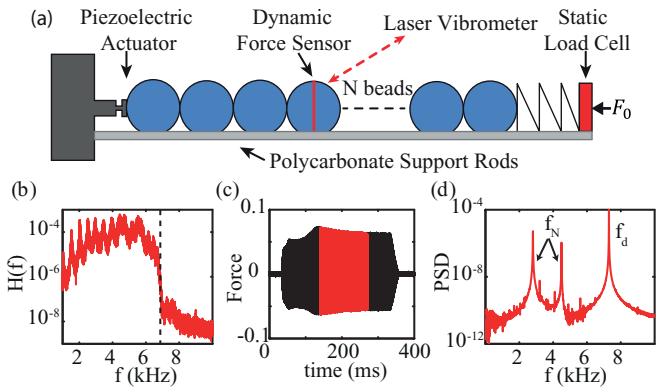

FIG. 1. (Color online) (a) Schematic of the experimental setup where the chain's length is varied between 1 and 50 beads. For one and two bead systems there was no embedded sensor. (b)–(d) The experimental bifurcation dynamics in a 15 bead chain statically compressed at 8 N and driven at 7.3 kHz. (b) The linear transfer function measured using a white noise excitation. The dotted line at 6.8 kHz indicates the band cutoff frequency measured at the half power point of the last peak. The drive frequency (7.3 kHz) for the force time series in (c) is therefore in the band gap. (c) The force time series measured at the end of the chain shows how the bifurcation results in the amplitude growth and stabilization. (d) The power spectral density (PSD) of the red portion of the force signal in (c) shows that energy is transferred from the drive frequency, $f_d = 7.3$ kHz, to two new frequencies f_N. We study how this bifurcation results from the finite size of a 1D system.

In this paper, we explore the nonlinear bifurcations that result from a system's finite size. We motivate the research by showing a typical bifurcation in a chain of 15 beads in Figs. 1(b)–1(d). Figure 1(b) shows the linear transmission band and the frequency band cutoff as a dotted line at 6.8 kHz. When driving the system at 7.3 kHz above a threshold amplitude, the oscillations grow and energy is transferred from the drive frequency to new frequencies. A stable quasiperiodic state is reached. The new frequencies and amplitudes depend sensitively on the drive frequency. Even though the system is driven in the stop band, energy can still propagate through the lower frequency modes. Because the dynamics for systems with many degrees of freedom are quite complex, we observe a slightly different result (i.e., the stable amplitudes and frequencies) for each experimental run. This means that the amplitude of the bifurcation and the newly generated frequencies depend sensitively on the initial compression. To understand the bifurcation structure governing this energy transfer, we start by studying smaller systems, i.e., a single bead oscillator and a two bead system, and then proceed to larger chains. The goal of this study is to understand the energy transfer of signals above the band gap to lower frequency modes that results from bifurcations. The systems of one and two beads illustrate the fundamental physics of the bifurcations and explain the dynamics present in larger systems. Therefore we build up from these two specific systems.

III. NUMERICAL SETUP

We model the dynamics of the granular chain using N coupled second order differential equations representing the motion of the particles. Accordingly, the ith sphere's displacement u_i from its equilibrium position can be described as

$$\begin{aligned} m\ddot{u}_1 &= A_{\mathrm{act}}[\delta_{\mathrm{act}} + B\cos(2\pi f t) - u_1]_+^{3/2} \\ &\quad - A\,(\delta_0 + u_1 - u_2)_+^{3/2} - m\dot{u}_1/\tau_d, \\ m\ddot{u}_i &= A\,(\delta_0 + u_{i-1} - u_i)_+^{3/2} \\ &\quad - A\,(\delta_0 + u_i - u_{i+1})_+^{3/2} - m\dot{u}_i/\tau_d, \\ m\ddot{u}_N &= A\,(\delta_0 + u_{N-1} - u_N)_+^{3/2} - F_0 - m\dot{u}_N/\tau_d, \end{aligned} \quad (1)$$

where $(s)_+$ takes the value of s if $s > 0$ and the value of 0 if $s \leqslant 0$ which signifies that adjacent particles are not in contact (gaps open). Here, m is the mass of the bead, $A = E\sqrt{2R}/[3(1-\upsilon^2)]$ is the constant in the Hertz interaction law [25], with the geometric and material properties defined above. The initial compression F_0 applied by the soft spring results in an initial static overlap δ_0 defined by Hertz's law $F_0 = A\,\delta_0^{3/2}$ [14]. The first bead's equation of motion is modified to reflect the harmonic drive and the contact between sphere and actuator, $A_{\mathrm{act}} = \sqrt{2}A$, modeled as a moving wall. The last bead's equation is modified to reflect the experimental boundary condition, a spring with force F_0. The equations of motion include a viscous on-site dissipation, τ_d. There is a slight variation around this value in the dissipation constant between experimental runs. We attribute this to change in the effect of the contact between the last bead and spring. To account for this, the dissipation

coefficient is calculated by fitting for each experiment's linear resonance response. It is important to note that these equations can be nondimensionalized leaving three critical parameters, the drive frequency, the drive amplitude, and the dissipation. All the numerical figures are plotted in nondimensional units to enhance readability.

For the analysis, we use a single shooting continuation algorithm and a Newton method to find periodic limit cycles in phase space [26]. The method computationally integrates the equations of motions and obtains a periodic solution with its associated Floquet multipliers (FMs), λ_j. The FMs are complex valued, and their magnitude can be used to study the linear stability of the solutions. In the case of dissipative lattices, the FMs originally lie on a circle of radius $e^{-1/(2\tau f_d)}$ [27]. Bifurcation instabilities result when the FMs collide and one leaves the unit circle, $|\lambda_i| > 1$. In this case, energy of the system is transferred from the drive frequency to nonlinear modes of the system at new frequencies. The argument of the complex FM gives us the new frequencies, $f_N = \frac{\mathrm{Arg}(\lambda_i)}{2\pi} f_d$.

IV. RESULTS AND DISCUSSION

At small drive amplitudes, $B/\delta_{\mathrm{act}} \ll 1$, the system's nonlinearity can be ignored and the response is nearly harmonic. However, as the drive amplitude increases, the system becomes nonlinear. The nonlinearity of a system can be described as either softening or stiffening depending on whether the maximum frequency response moves down or up as the drive amplitude is increased. Figure 2(a) shows the experimental nonlinear softening of the mode of a single bead. As the amplitude of the drive is increased the response becomes asymmetric, bending to lower frequencies (i.e., a softening nonlinear potential), deviating from the classic linear Lorentzian response. The amplitude dependent mode profile that we observe here is a property of nonlinear oscillators commonly studied in the driven damped Duffing oscillator [3]. Figure 2(b) shows experimental data demonstrating a similar nonlinear softening response for each of the modes of a two bead system. This mode softening is important to the dynamics at higher amplitudes after the bifurcation occurs. It illustrates the nonlinear behavior of the system and explains asymmetry seen later in Fig. 5. The numerical counterparts to Figs. 2(a) and 2(b) are shown in Figs. 2(c) and 2(d). The nonlinear softening of the system is qualitatively similar in these plots. We notice a significant difference in the quantitative amplitudes observed for the nonlinear softening. We believe the quantitative difference in the measured and computed values could be due to one or a combination of many effects. Some of these could include the variation of the surface roughness of the sphere, frictional nonlinearities that become important at low amplitudes, or inaccuracy in measurement and excitation techniques at these extremely low amplitudes. A further investigation of this deviation from the Hertzian contact law at low drive amplitudes would be an interesting future study. However, the key result for our study is the observation that the dynamics are nonlinear, and that there is a softening of the resonance, i.e., the maximum of the frequency moves to lower values as the drive amplitude is increased. We discuss later how this softening could account for the asymmetry bifurcations in frequency.

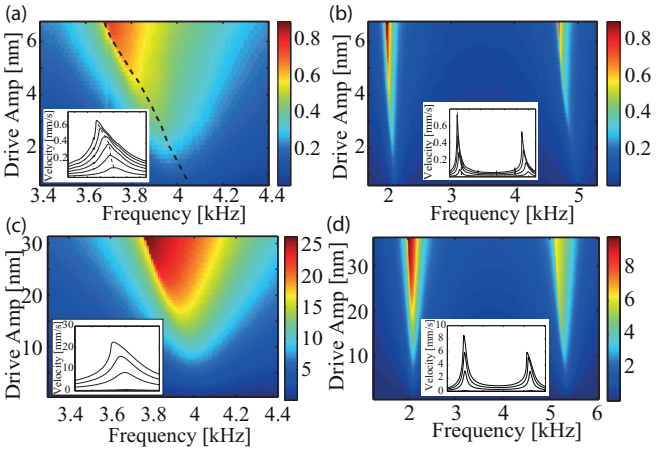

FIG. 2. (Color online) Color maps of the experimentally measured rms velocity (mm/s) of single bead (a) and two bead (b) systems as a function of the drive amplitude and frequency. The velocity is measured in the second bead for the two bead system. The dotted line in (a), which starts at 4.05 kHz for low amplitudes and decreases in frequency at higher amplitudes, indicates the maximum of the resonance at each drive amplitude. This clearly displays the mode softening to lower frequencies as the amplitude of the excitation increases. The insets show cross sections at selected drive amplitudes. The horizontal axis of the insets is the same frequency axes as each corresponding panel. The asymmetry and the mode softening is a result of the nonlinear Hertzian contact interaction. The measurements are taken using a lock-in amplifier to reduce noise. In addition, the low amplitude response is used to estimate the dissipation coefficients used in the one and two bead computational results. Panels (c) and (d) are the computational counterparts to (a) and (b). The system depends sensitively on the initial compression F_0 and the diagrams are fit to have the same linear (low amplitude) frequency as the experimental plots. This corresponds to a 8.67 N static compression for the single bead and 4.36 N for two beads.

We are interested in changes of the wave dynamics before and after the bifurcation. Figure 3 shows an experimentally measured bifurcation in a single bead system when the particle is driven at approximately twice the natural frequency. Initially, a stable harmonic solution develops [Fig. 3(a)], but as the drive amplitude is increased, the velocity sharply increases and the dynamic response changes [Fig. 3(b)]. The data in Fig. 3(c) show a sudden jump in the dynamic response at a critical drive amplitude, $B_{\mathrm{crit}} = 0.07\,\mu$m. The power spectral density (PSD) [see Figs. 3(d) and 3(g)] shows that this solution went from being composed of the single drive frequency to being dominated by a subharmonic, $f_d/2$. Figure 3(e) shows the Poincaré section change from a single grouping of points to two distinct groups, indicative of a subharmonic bifurcation [28]. After the bifurcation, approximately 20 times more energy is transferred to the bead, indicating much more efficient coupling between the particle chain and the actuator. In addition, the increase in the oscillation amplitude of the bead, as a result of the bifurcation, depends on the drive frequency. Figure 3(f) shows the computationally calculated hysteresis diagram that corresponds to the experiment. The disagreement observed in the predicted and measured velocity amplitudes can be explained by uncertainty in measurements

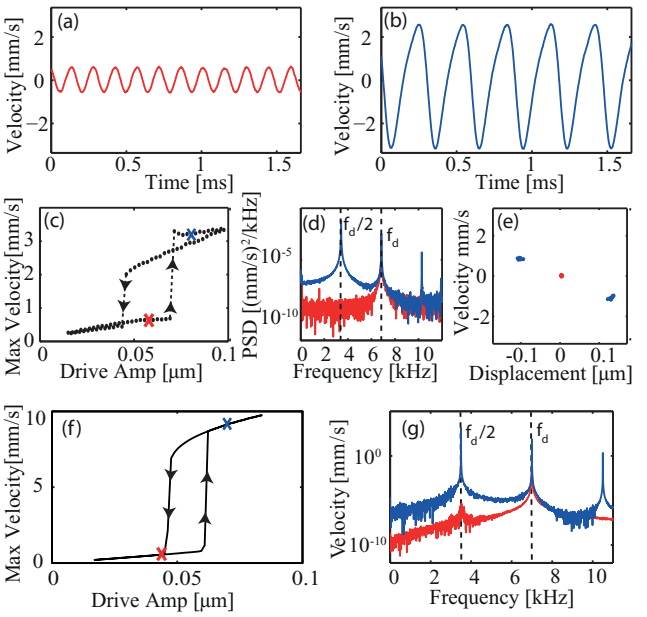

FIG. 3. (Color online) The experimental nonlinear resonance and bifurcation behavior of a single bead driven at 6.85 kHz. (a),(b) The velocity of the bead (a) before and (b) after the bifurcation. (c) The maximum velocity measured at each drive amplitude. The two crosses indicate the drive amplitudes for the time series in (a), red lower left cross, and (b) right lower left cross. (d) The corresponding PSD of two time series, showing the dominant subharmonic frequency at $f_d/2$ for the excitation above the bifurcation amplitude. The dotted lines indicate the drive frequency (right) and new subharmonic (left) frequency. (e) the Poincaré section of the dynamics of the bead before (red, central points) and after (blue, side points) the bifurcation. The splitting of the section from one point to two points is characteristic of a period doubling subharmonic bifurcation. Panels (f) and (g) are the computational plots that correspond to the experimental panels (c) and (d). (g) The PSD clearly shows that a subharmonic bifurcation occurs after the critical amplitude is crossed.

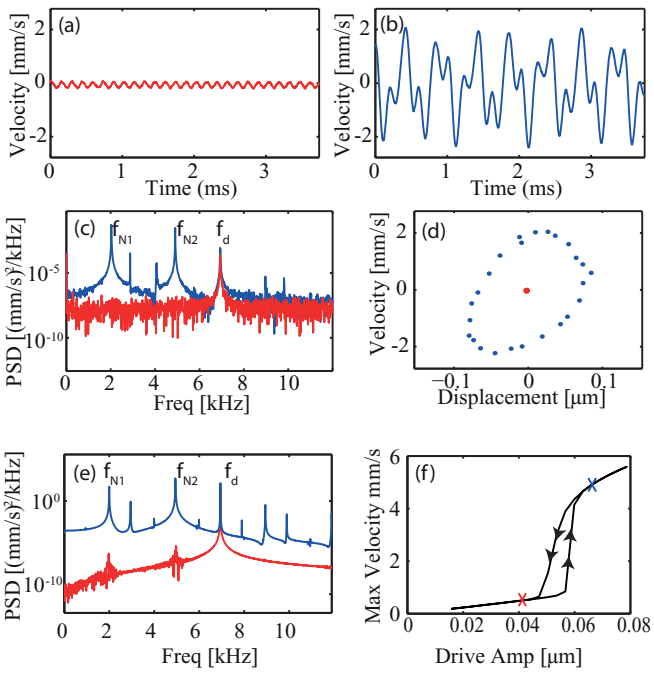

FIG. 4. (Color online) Experimental nonlinear resonance and quasiperiodic bifurcation behavior in a system of two beads driven at 6.94 kHz. (a),(b) The velocity of the second bead (a) before and (b) after the bifurcation. (c) The corresponding PSD of two time series, showing the new frequencies f_{N1} and f_{N2} supported by the nonlinearity of the system, where $f_{N1} + f_{N2} = f_d$. The PSD of the time series clearly shows that energy is transferred from the drive frequency f_d to the two new frequencies. (d) Poincaré sections of the dynamics of the second bead before (red, central point) and after (blue, surrounding points) the bifurcation. This Poincaré shows the classic intersection of a torus and a plane for quasiperiodic dynamics. The finite number of points is due to the finite length of the signal. (e) The PSD of the computational time series taken at the drive amplitudes indicated in (f) and using the same parameters as measured during the experimental runs. The lower left cross indicates the drive amplitude chosen before the bifurcation, and the upper right cross is at a higher amplitude after the bifurcation.

of the static compression applied to the chain, even though all qualitative features of the bifurcation are maintained.

In longer chains, there is more than one natural frequency, and therefore the system can undergo bifurcations resulting in both subharmonic or quasiperiodic dynamics. When the drive frequency is a multiple of a linear mode's frequency, a subharmonic bifurcation emerges, and the dynamics are qualitatively similar to the results shown for a single bead. However, when the drive frequency is near the sum of the system's two natural frequencies, quasiperiodic dynamics may arise. Figure 4 shows the response of a two bead system that goes from a sinusoidal response [Fig. 4(a)] to a solution that is quasiperiodic [Fig. 4(b)]. Quasiperiodic dynamics occur because the ratios between the drive frequency f_d and new frequencies f_{N1} and f_{N2} are not necessarily rational. Figure 4(c) shows the PSDs of the signals, and illustrates the transfer of energy to the two lower modes. Figure 4(d) shows the Poincaré section of the second bead. It contains points forming a closed curve coming from the intersection of the torus flow in phase space (characteristic of quasiperiodic dynamics) with a plane. In summary, the system goes through a bifurcation in which the dynamics drastically change. There is an order of magnitude change in the amplitude, the total energy transferred to the system, and fraction of energy localized around the drive frequency. To confirm the quasiperiodic behavior, we also performed a computational integration using the same parameters as in the experiment. Figure 4(e) shows the power spectral density before and after the critical amplitude of the bifurcation. The values are shown in the hysteresis plot of Fig. 4(f). The dynamics agree quite well, and the qualitative disagreements can be attributed to uncertainty in the static compression and reconfigurations of the system coming from misalignment of the spheres during each experimental run.

The analysis for one and two bead systems illustrates the two fundamental types of bifurcations that occur in granular chains. Figure 5 shows how the bifurcations depend on the different parameters of the system, i.e., drive amplitude and drive frequency. We observed that these bifurcations occur in certain areas of the parameter space and call these regions tongues, due to their similarity with parametric tongues.

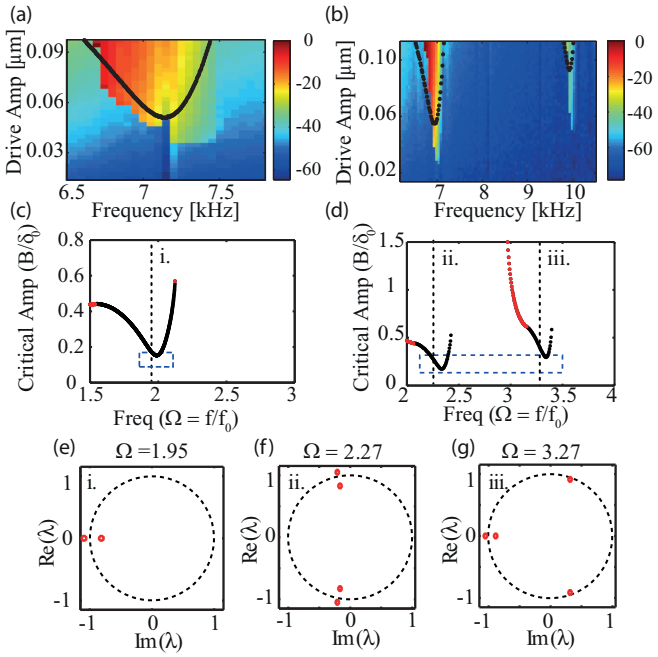

FIG. 5. (Color online) The experimentally measured bifurcation tongues observed in (a) one bead and (b) two bead systems. The color scale corresponds to maximum velocity amplitude (dB), and it demonstrates that as the mode moves further from its linear frequency, the change in dynamics becomes more drastic. The numerically calculated tongue edge is plotted directly on top of the experimental data as closely spaced solid black dots. Panels (c) and (d) show the computational results for one and two bead chains, respectively (the units are nondimensional). The solid points indicate where a bifurcation has occurred (i.e., a FM has left the unit circle). Red points (at the higher frequency portions for each tongue) indicate gaps have opened between beads. The dashed rectangles indicate the parameter range for the experimental measurements in (a) and (b). The vertical dotted lines correspond to the Floquet diagrams in (e)–(g). We show the unit circle to guide the eye.

This region indicates that, where a sharp transition in the dynamics occurs, the stable solution goes from sinusoidal to either subharmonic or quasiperiodic. The tongues are centered around the multiples and sums of the linear mode frequencies in each system. Numerically we can determine where to sweep these frequencies by solving the eigenvalue problem associated with the equations of motion (1), and experimentally we measure the linear mode frequencies using a broad range frequency sweep. We start by showing the experimental and computational bifurcation tongues of a one and two bead system and then proceed to larger systems. The edge of the tongue shows the edge of a stable harmonic solution. Above the critical drive amplitude the system exhibits either subharmonic or quasiperiodic dynamics.

Figure 5(a) shows the experimentally observed nonlinear tongue for a single bead oscillator. Here, the entire tongue is characterized as subharmonic. The minimum of this region corresponds to twice the frequency of the linear mode. The disagreement between the minimum of the tongue in Fig. 5(a) (7.4 kHz) and twice the linear frequency, 4.0 kHz shown in Fig. 2(a), is due to different static compressions between runs. The linear frequency measurements were taken at approximately 8 N compression, while the bifurcation is measured at approximately 4 N. On top of the experimental results, we also plot the computationally computed tongue edge as a black dotted line. The tongue is asymmetric due to the modes softening to lower frequencies (Fig. 2). As amplitudes of the oscillations increase, the natural frequencies decrease. This causes the tongue in Fig. 5(a) to bend towards lower frequencies. In addition, the color scale shows that the bifurcation becomes more drastic as the mode bends further from its linear natural frequency. Figure 5(c) shows the computationally calculated bifurcation tongue for a single bead (with the experimentally investigated region indicated with the dashed blue rectangle). The quantity f_0 used to nondimensionalize the frequency is the linear mode frequency. Here it is clear the minimum is at 2, or twice this frequency. This is because the drive frequency determines how far apart the nonlinear modes must move in frequency. If the drive frequency is chosen as the minimum in the tounge, it is already a multiple of the linear mode frequency. In the context of the Floquet multipliers, the multipliers start on top of each other. If a frequency slightly lower or above the minimum is chosen, the nonlinear modes decrease or increase in frequency to be a multiple of the drive frequency. The Floquet multipliers must first move before colliding. Therefore the bifurcation occurs most easily at a multiple of the linear mode frequency, leading to a minimum at this point. The solid points in Figs. 5(a)–5(d) are computed using a parameter continuation, and they correspond to the pairs of the driving frequency and amplitude at which FMs leave the unit circle, an indicator of the existence of bifurcations. In these plots, the asymmetry becomes clear. Points in red indicate that gaps are opening, which explains why the shape of the tongue changes; the dynamics at this point go from weakly to strongly nonlinear. The units are shown in nondimensional units to stress that the onset of this nonlinear bifurcation may occur at seemingly small drive amplitudes, at a fraction of the static overlap of the chain.

For two beads [Figs. 5(b) and 5(d)] we see two tongues: one at the sum of the two mode frequencies, 7 kHz, and one at twice the higher mode's frequency, 9.8 kHz. The tongue associated with the sum is characterized by quasiperiodic bifurcation dynamics, whereas the tongue at twice the mode's frequency is subharmonic. A single slice from the quasiperiodic tongue was previously shown in Fig. 4, where the frequency is fixed and the drive amplitude is quasistatically increased. It is important to note that our computations predict that high amplitude subharmonic and quasiperiodic stable solutions exist despite gaps opening, i.e., gaps openings do not directly lead to chaotic dynamics. In this case, the dynamics are nonsmooth yet still periodic. While this is somewhat surprising, the possibility of such dynamics is supported by the nonsmooth periodic solutions that have previously been observed in granular chains at the uncompressed limit [20,29]. Figures 5(e)–5(g) show a representative of the FMs calculated for each tongue. If the FMs leave the unit circle on the negative real axis, it indicates a subharmonic bifurcation, and otherwise quasiperiodic dynamics. These simulations confirm the subharmonic and quasiperiodic dynamics observed experimentally for each tongue in Figs. 3 and 4 in which we increase the amplitude

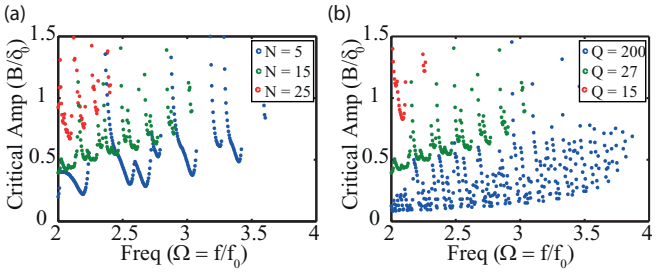

FIG. 6. (Color online) The interplay between finite size and dissipation. The points indicate a critical bifurcation amplitude, calculated using numeric. In (a) we hold the dissipation of the system constant ($Q = 27$) and vary the size of the system. The individual tongues begin to overlap and the bifurcations begin to occur at higher amplitudes. In (b) the finite size ($N = 15$) is held constant and the dissipation is varied. For lower dissipations the bifurcation tongues start at lower amplitude. All units shown are nondimensional.

entering the nonlinear tongue region. The critical driving amplitude for bifurcation shows a good agreement in the experimental and computational results for one and two beads.

The results from one and two beads help us understand the dynamics that can take place in larger systems. Any linear combination or multiple of the mode frequencies can result in a bifurcation tongue, and for slightly larger systems the number of combinations quickly grows and so does the number of tongues. In lattices of longer length, the attenuation band that forms prevents the propagation of signals above a certain frequency. However, the previous study of a one and two bead system shows that energy can be transferred through lower frequencies. When this happens in longer chains, the attenuation band will no longer reflect all of the incident signal, but instead energy will be transferred to lower frequencies that can still propagate.

In Fig. 6, we study the effect of the size of the system and the losses of the system on the existence and the structure of these bifurcation tongues. In particular, Fig. 6(a) shows the effect of increasing the size of the system for a given amount of losses that correspond to the nondimensional quality factor ($Q = 27$) of the single bead system. For five beads there are already many more tongues, but they can still be distinguished. For 15 beads the tongues can no longer be distinguished and the amplitude, at which the bifurcations happen, is larger. This explains the sensitivity of the bifurcation that we observed for 15 beads shown and discussed in Fig. 1. Finally, for 25 beads we barely see the tongue structure while for systems of 40 and 50 beads we observe no bifurcations even when driving up to 1.5 times the static overlap. Figure 6(b) shows the effect of the losses for a given chain length ($N = 15$). As the dissipation is decreased (increasing quality factor) the system can much more easily bifurcate. In both panels, we also observe that as the driving frequency increases, the appearance of bifurcations happens at larger driving amplitudes. In conclusion, as the system gets longer and/or more lossy, the bifurcations happens at larger driving amplitude and at some point they are no longer present. Thus, there is an important interplay between the losses and the length of the system that leads to the existence or not of bifurcations and thus to the nonlinear energy transfer between phonon modes.

This could be explained from the perspective of FM as follows: The bifurcations are associated with what is called oscillatory instability, which arises from the collision of two Floquet multipliers and the associated spatially extended eigenvectors, a well-known finite-size effect. When this collision occurs, if a FM leaves the unit circle, then the solution is unstable and grows. The magnitude of this multiplier is also a measure of the strength of the instability and how quickly it grows. As discussed in Ref. [17] the strength of such instabilities depends on the system size. In particular, when the size of the system is increased, the magnitude of such instabilities weakens uniformly. In other words, the unstable FMs become smaller in magnitude as the system size grows. Simultaneously, the number of such instabilities increases with system size due to the increasing density of colliding Floquet multipliers. Eventually, these instabilities vanish in the limit of an infinitely large system. Since in Hamiltonian lattices, all the FMs must lie on the unit circle, collisions result in their departure from the unit circle and are directly associated with instabilities. However, this is not the case for the driven-damped lattices. As we mentioned above, for a linearly stable periodic solution all the FMs lie on a circle of radius, $e^{-1/(2\tau f_d)}$, which is smaller than 1. As the dissipation increases, the Floquet multipliers have a smaller magnitude and the instability must be strong enough to allow the FM to completely leave the unit circle. Thus, it is possible for FMs to collide but still not exit the unit circle. This is due to the weak strength of the oscillatory instabilities, which becomes weaker as the size of the lattice becomes larger. Therefore, at longer lengths there is no manifestation of bifurcations and thus no nonlinear energy transfer to the lower frequency phonon modes. This means that in shorter "periodic" systems, even relatively weak nonlinearities may become important. The bifurcations in our system occur at much lower drive amplitudes than we had previously thought, and at amplitudes where the dynamics are still weakly nonlinear and smooth. When the dynamics are weakly nonlinear the Hertzian potential can be expressed as a polynomial expansion. Therefore, periodic materials with a coupling interaction that is not strictly linear, but instead has an asymmetric or nonlinear content, may exhibit similar bifurcation dynamics. This could lead to the failure of linear approximations in other finite length systems due to weak nonlinearities.

Furthermore, we observe that at higher frequencies the bifurcations happen at higher amplitudes. This could be explained in two ways. First, the linear on-site damping in a lattice results in an increased effective damping of the higher frequency phonon modes (see for example Chap. 6 of Ref. [1]). This is evident in our experiments for example in Fig. 1(b), where one can see that close to the band edge, the linear response flattens out into a low pass filter and there are no longer distinct resonances. As a result, bifurcations at higher drive frequencies, which are due to the excitation of a pair of high frequency phonon modes, are more difficult to appear. Second, this can also be interpreted as a consequence of the evanescent wave breaking down [30]. The further the excitation frequency is above the band edge, the more the evanescent wave corresponding to this frequency is localized. The evanescent wave does not penetrate as deeply into the lattice at higher frequencies and the interaction between the

evanescent wave and the extended modes of the crystal become increasingly smaller. This interaction becomes smaller as the chain length increases (longer extended modes) and as the dissipation increases (weaker evanescent waves in amplitude). Correspondingly, the bifurcation instabilities occur at larger amplitudes.

V. CONCLUSION

We have experimentally and computationally investigated the nonlinear resonance phenomena and the resulting bifurcation instabilities in finite, monodisperse, harmonically driven 1D granular chains, taking into account losses. The nonlinear bifurcation tongues arise from the finite size of the discrete system, and the tongues' shapes depend on the type of nonlinear coupling in the lattice. This dynamic response demonstrates how energy can be transferred from a single excitation signal to other frequencies fundamental to a material lattice. The nonlinear interactions in granular chains provide a completely passive mechanical mechanism to control the transmitted frequency spectrum. The structural stability and nonlinear bifurcation dynamics of homogeneous granular chains may be used in multifunctional material design where previous solutions were limited to actively controlled mechanical systems. The findings of this paper should be considered in the design of new devices consisting of nonlinear finite lattices, for example, for amplitude dependent filtering applications or for mechanical structures aiming at an enhanced frequency control of propagating waves.

ACKNOWLEDGMENTS

J.L. and C.D. acknowledge support from US-AFOSR (Grant No. FA9550-12-1-0332). G.T. acknowledges financial support from FP7-PEOPLE-2013-CIG (Project No. 618322 ComGranSol). We thank M. Serra Garcia for his support in experiments.

[1] P. A. Deymier, *Acoustic Metamaterials and Phononic Crystals* (Springer, Heidelberg, New York, 2013).
[2] R. V. Craster and S. Guenneau, *Acoustic Metamaterials: Negative Refraction, Imaging, Lensing and Cloaking* (Springer, Heidelberg, New York, 2012).
[3] A. Nayfeh and D. Mook, *Nonlinear Oscillations* (John Wiley & Sons, New York, 1979).
[4] T. Von Karman, The engineer grapples with nonlinear problems, Bull. Am. Math. Soc. **46**, 615 (1940).
[5] P. E. Powers, *Fundamentals of Nonlinear Optics* (Taylor & Francis, Boca Raton, Florida, 2011).
[6] N. Boechler, G. Theocharis, and C. Daraio, Bifurcation-based acoustic switching and rectification, Nat. Mater. **10**, 665 (2011).
[7] B. Liang, X. S. Guo, J. Tu, D. Zhang, and J. C. Cheng, An acoustic rectifier, Nat. Mater. **9**, 989 (2010).
[8] R. A. Guyer and P. A. Johnson, *Nonlinear Mesoscopic Elasticity: The Complex Behaviour of Rocks, Soil, Concrete* (Wiley, Weinheim, 2009).
[9] F. Geniet and J. Leon, Nonlinear supratransmission, J. Phys.: Condens. Matter **15**, 2933 (2003).
[10] R. Khomeriki, S. Lepri, and S. Ruffo, Nonlinear supratransmission and bistability in the Fermi-Pasta-Ulam model, Phys. Rev. E **70**, 066626 (2004).
[11] A. B. Togueu Motcheyo, C. Tchawoua, and J. D. Tchinang Tchameu, Supratransmission induced by waves collisions in a discrete electrical lattice, Phys. Rev. E **88**, 040901 (2013).
[12] F. Geniet and J. Leon, Energy transmission in the forbidden band gap of a nonlinear chain, Phys. Rev. Lett. **89**, 134102 (2002).
[13] G. Theocharis, N. Boechler, and C. Daraio, in *Acoustic Metamaterials and Phononic Crystals* (Springer, New York, 2013), pp. 217–251.
[14] V. Nesterenko, *Dynamics of Heterogeneous Materials* (Springer, New York, 2001).
[15] G. Theocharis, M. Kavousanakis, P. G. Kevrekidis, C. Daraio, M. A. Porter, and I. G. Kevrekidis, Localized breathing modes in granular crystals with defects, Phys. Rev. E **80**, 066601 (2009).
[16] N. Boechler, G. Theocharis, S. Job, P. G. Kevrekidis, M. A. Porter, and C. Daraio, Discrete breathers in one-dimensional diatomic granular crystals, Phys. Rev. Lett. **104**, 244302 (2010).
[17] J. L. Marín and S. Aubry, Finite size effects on instabilities of discrete breathers, Physica D: Nonlin. Phenom. **119**, 163 (1998).
[18] J. Cabaret, V. Tournat, and P. Béquin, Amplitude-dependent phononic processes in a diatomic granular chain in the weakly nonlinear regime, Phys. Rev. E **86**, 041305 (2012).
[19] C. Hoogeboom, Y. Man, N. Boechler, G. Theocharis, P. G. Kevrekidis, I. G. Kevrekidis, and C. Daraio, Hysteresis loops and multi-stability: From periodic orbits to chaotic dynamics (and back) in diatomic granular crystals, Europhys. Lett. **101**, 44003 (2013).
[20] K. Jayaprakash, Y. Starosvetsky, A. Vakakis, M. Peeters, and G. Kerschen, Nonlinear normal modes and band zones in granular chains with no pre-compression, Nonlin. Dyn. **63**, 359 (2011).
[21] E. B. Herbold, J. Kim, V. F. Nesterenko, S. Y. Wang, and C. Daraio, Pulse propagation in a linear and nonlinear diatomic periodic chain: Effects of acoustic frequency band-gap, Acta Mech. **205**, 85 (2009).
[22] V. Tournat, C. Inserra, and V. Gusev, Non-cascade frequency-mixing processes for elastic waves in unconsolidated granular materials, Ultrasonics **48**, 492 (2008).
[23] J. R. Davis and A. I. H. Committee, *Metals Handbook* (ASM International, Materials Park, OH, 1998).
[24] S. Job, F. Melo, A. Sokolow, and S. Sen, How Hertzian solitary waves interact with boundaries in a 1D granular medium, Phys. Rev. Lett. **94**, 178002 (2005).
[25] H. Hertz, Über die berührung fester elastischer Körper (On the contact of rigid elastic solids). In *Miscellaneous Papers*, Jones and Schott, edited by J. reine und angewandte Mathematik 92 (MacMillan, London, 1896), p. 156 English translation: Hertz, H.
[26] G. Theocharis, N. Boechler, P. G. Kevrekidis, S. Job, M. A. Porter, and C. Daraio, Intrinsic energy localization through discrete gap breathers in one-dimensional diatomic granular crystals, Phys. Rev. E **82**, 056604 (2010).

[27] J. L. Marín, F. Falo, P. J. Martínez, and L. M. Floría, Discrete breathers in dissipative lattices, Phys. Rev. E **63**, 066603 (2001).

[28] S. H. Strogatz, *Nonlinear Dynamics and Chaos: With Applications to Physics, Biology, Chemistry, and Engineering* (Westview, Boulder (Colorado), 1994).

[29] J. Lydon, K. R. Jayaprakash, D. Ngo, Y. Starosvetsky, A. F. Vakakis, and C. Daraio, Frequency bands of strongly nonlinear homogeneous granular systems, Phys. Rev. E **88**, 012206 (2013).

[30] J. Leon, Nonlinear supratransmission as a fundamental instability, Phys. Lett. A **319**, 130 (2003).